pISSN 1598-2998, eISSN 2005-9256

Cancer Res Treat. 2019;51(1):345-356

https://doi.org/10.4143/crt.2018.089

Original Article

Open Access

Longitudinal Assessment of Intravoxel Incoherent Motion Diffusion Weighted Imaging in Evaluating the Radio-sensitivity of Nasopharyngeal Carcinoma Treated with Intensity-Modulated Radiation Therapy

Youping Xiao, MD[1]
Ying Chen, BS[1]
Yunbin Chen, MD[1]
Zhuangzhen He, MS[1]
Yiqi Yao, MS[1]
Jianji Pan, MD[2]

Departments of [1]Radiology and [2]Radiation Oncology, Fujian Cancer Hospital & Fujian Medical University Cancer Hospital, Fuzhou, China

Correspondence: Yunbin Chen, MD
Department of Radiology, Fujian Cancer Hospital & Fujian Medical University Cancer Hospital, Fuzhou, China
Tel: 86-13950301116
Fax: 86-59183660063
E-mail: Yunbinchen@126.com

Co-correspondence: Ying Chen, BS
Department of Radiology, Fujian Cancer Hospital & Fujian Medical University Cancer Hospital, Fuzhou, China
Tel: 86-15980213050
Fax: 86-59183660063
E-mail: Cheyne09@163.com

Received February 5, 2018
Accepted May 9, 2018
Published Online May 14, 2018

Purpose

Intravoxel incoherent motion diffusion-weighted imaging (IVIM-DWI) was evaluated regarding its ability to preliminarily predict the short-term treatment response of nasopharyngeal carcinoma (NPC) following intensity-modulated radiation therapy.

Materials and Methods

IVIM-DWI with 14 b-factors (0-1,000 sec/mm^2) was performed with a 3T MR system on 47 consecutive NPCs before, during (end of the 5th, 10th, 15th, 20th, and 25th fractions), and after fractional radiotherapy. IVIM parametrics (D, f, and D*) were calculated and compared to the baseline and xth fraction. Patients were categorized into responders and non-responders after radiotherapy. IVIM parametrics were also compared between subgroups.

Results

After fractional radiations, the D (except D_5 and D at the end of the 5th fraction) after radiations were larger than the baseline D_0 ($p < 0.05$), and the post-radiation D* (except D^*_5 and D^*_{10}) were smaller than D^*_0 ($p < 0.05$). f_0 was smaller than f_5 and f_{10} ($p < 0.001$) but larger than f_{end} ($p < 0.05$). Furthermore, greater D_5, D_{10}, D_{15}, and f_{10} coupled with smaller f_0, D^*_{20}, and D^*_{25} were observed in responders than non-responders (all $p < 0.01$). Responders also presented larger ΔD_{10}, Δf_{10}, ΔD^*_{20}, and δD^*_{20} than non-responders ($p < 0.05$). Receiver operating characteristic curve analysis indicated that the D_5, D^*_{20}, and f_{10} could better differentiate responders from non-responders.

Conclusion

IVIM-DWI could efficiently assess tumor treatment response to fractional radiotherapy and predict the radio-sensitivity for NPCs.

Key words
Intravoxel incoherent motion, Diffusion-weighted imaging, Nasopharyngeal carcinoma, Radiosensitivity, Intensity-modulated radiotherapy

Introduction

Among types of head and neck squamous cell carcinoma (HNSCC), nasopharyngeal carcinoma (NPC) is the most common and is highly prevalent in Southeast Asia and Southern China [1]. The majority of NPC was found to be non-keratinizing in endemic regions [2] and was highly sensitive to irradiation and chemotherapeutic drugs. The primary treatment regimen for NPCs is radiotherapy (RT) coupled with or without chemotherapy. However, there are limited effective non-invasive image modalities for the early prediction of tumor response to chemoradiotherapy (CRT).

Intensity-modulated radiation therapy (IMRT) for NPC has been reported to provide satisfactory outcomes compared to other RT techniques [3,4]. For advanced diseases, CRT shows a better prognosis than RT alone, especially sequential CRT and concurrent chemoradiotherapy (CCRT)

[5-7]. In particular, studies reported higher survival rates in patients undergoing CCRT than sequential CRT [6,7]. Notably, radio-resistance, tumor recurrence, and the development of distant metastases remain the contributing reasons for treatment failure. In this regard, an optimal imaging regimen is critical for early assessment of radiosensitivity of tumor. A valid imaging modality was explored to assess the treatment responses of NPCs.

Routine magnetic resonance imaging (MRI) currently provides a better soft tissue contrast and spatial resolution in evaluating the extent of primary nasopharynx tumor and positive cervical nodes and also plays a conventional role in assessing tumor's response to CRT. However, morphological images only reveal macroscopic changes in tumor size that may not be apparent, and the initial treatment and characterization of immediate therapeutic effects could be limited. Recent studies primarily focused on the functional treatment response of tumors by various MRI techniques. For instance, diffusion-weight imaging (DWI) measures and characterizes the thermal motion of water molecules. In particular, the apparent diffusion coefficient (ADC) has been validated as a potential imaging biomarker to identify tumor treatment response [8]. However, ADC is calculated based on a mono-exponential model that reflects the combined effects of diffusion and perfusion [9].

In contrast, intravoxel incoherent motion (IVIM), which was initially described by Le Bihan et al. in 1986 [9], is a bi-exponential model to separately quantify tissue diffusion and perfusion [10]. In recent decades, IVIM-DWI has gained attentions due to its effective diagnostic capability in tumors, including those of the head and neck [11,12]. Moreover, IVIM parametrics have been correlated with clinical staging [13] as well as the treatment response of HNSCC [14,15]. Our previous study validated the potential value of IVIM-DWI in predicting the early treatment response of neoadjuvant chemotherapy (NAC) in local to regionally advanced NPCs [16]. Nevertheless, the assessment of IVIM-DWI regarding the radio-sensitivity of NPCs is yet to be explored. Since early prediction of treatment response through IVIM-DWI might arise significant impacts on patient-care planning and treatment regimens, the objective of this study is to evaluate the clinical value of IVIM-DWI in predicting the treatment response to IMRT in NPCs.

Materials and Methods

1. Patients and treatment

1) Patient enrollment

A cohort of 64 consecutive NPC patients was enrolled between May 2015 and August 2016. The inclusion criteria were as follows: (1) histopathological diagnosis of NPC, (2) no pregnancy, (3) no contraindications for magnetic resonance (MR) scanning, (4) no allergies to contrast agents of gadolinium (Gd), (5) a treatment plan of IMRT with or without chemotherapy, and (6) complete acquisition of all follow-up IVIM-DWI.

Forty-seven subjects who met the above criteria were included. The remaining 17 cases were excluded from this study for the following reasons: three due to the severe distortion and artifacts of images, 10 failed to complete all follow-up IVIM-DWI, and four missed the MR examination after CRT. Four NPC were classified as pathological type World Health Organization (WHO) II, and the remaining 43 were WHO III. According to the staging criteria of NPC of The American Joint Committee on Cancer [17], one, eight, 20, and 18 cases were staged I, II, III, and IV, respectively. Table 1 summarized the clinical characteristics of the recruited patients.

2) Treatment regimens

All recruited patients were treated with definitive IMRT with or without chemotherapy. The detailed description of IMRT has been published previously [18]. The primary NPC tumor and its surrounding invasive regions were defined as gross target volume-tumor (GTV-T), the GTV-T–planning target volume (PTV) (95%V) exposure dose was 6,600-7,425 cGy/30-33 fractions (period, 6-7 weeks), and the fractional irradiation dose was 225 cGy. The surrounding region of 5-10 mm beyond GTV-T was established as clinical target volume (CTV) 1, and the CTV1-PTV (95%V) exposure dose was 6,000-6,270 cGy/30-33 fractions (period, 6-7 weeks), and the fractional dose was of 190-200 cGy. However, the region of the suspected and positive cervical nodes were identified as CTV2, and the CTV2-PTV (95%V) exposure dose was 5,400-5,610 cGy/30-33 fractions (period, 6-7 weeks); the fractional irradiation dose was of 170-180 cGy.

A total of 41 cases (87.23%) also received the platinum-based chemotherapy. The detailed regimens of chemotherapy were as follows (Table 1): 35 cases (74.46%) of NAC, including 26 cases of cisplatin plus Taxol and nine cases of cisplatin plus gemcitabine; six cases (12.77%) of CCRT by applying cisplatin alone (from day 1 to 3 in 21-day cycles);

Table 1. The clinical characteristics of recruited NPC patients

Characteristic	No. of cases (%)
Recruited patients	47
Male	33 (70.21)
Female	14 (29.79)
Age (yr)	
Median	48
Range	21-74
< 60	28 (59.57)
≥ 60	19 (40.43)
Pathological type[a)]	
WHO III	43 (91.49)
WHO II	4 (8.51)
Clinical stage[b)]	
Stage I (T1N0M0)	1 (2.13)
Stage II (T1-2N1M0/T2N0-1M0)	8 (17.02)
Stage III (T1-2N2M0/T3N0-2M0)	20 (42.55)
Stage IV (T4N0-2M0/T1-4N3M0/T1-4N0-3M1)	18 (38.30)
Treatment regimen	
IMRT alone	6 (12.77)
CCRT	6 (12.77)
NAC+IMRT	35 (74.46)

NPC, nasopharyngeal carcinoma; WHO, World Health Organization; IMRT, intensity-modulated radiation therapy; CCRT, concurrent chemoradiotherapy; NAC, neoadjuvant chemotherapy. [a)]The WHO pathological types of NPC [5], [b)]The staging criteria of NPC is according to the seventh edition of American Joint Committee on Cancer [27,28].

the remaining six cases received RT alone. Patients with persistent or recurrent tumors after completing the initial treatments (IMRT alone or CRT) received salvage treatments (including intracavitary brachytherapy, surgery, and/or further adjuvant chemotherapy, etc.) when possible.

2. MRI protocols

1) Conventional MRI

Before initial treatments, head and neck MRI from the lower temporal lobe to the supraclavicular region were performed on a 3.0T MR system (Achieva, Philips Healthcare, Best, Netherlands). Conventional MRI protocols including these following sequences: (1) axial T1-weighted imaging-turbo spin-echo (T1WI-TSE): repetition time/echo time (TR/TE), 550/8.1 msec; field of view (FOV), 23 cm×23 cm; reconstruction matrix, 960×960; slice number, 36; thickness, 5 mm; gap, 1 mm; (2) axial T2-weighted imaging with short TI inversion recovery (T2WI-STIR): TR/TE, 6,888/70 msec; FOV, 23 cm×23 cm; matrix, 960×960; slice, 18; thickness, 5 mm; gap, 1 mm; (3) coronal T2WI-STIR: TR/TE, 2,327/63 msec; FOV, 23 cm×23 cm; matrix, 672×672; thickness, 5 mm; gap, 1 mm; (4) sagittal T1WI-TSE: TR/TE, 600/8.1 msec; FOV, 23 cm×23 cm; matrix, 768×768; thickness, 5 mm; gap, 1 mm; and (5) postcontrast-enhanced secquences of axial, sagittal, and coronal T1WI-TSE with spectral presaturation inversion recovery: TR/TE, 1,215/8.1 msec; flip angle, 90°; FOV, 23 cm×23 cm; matri, 960×960; thickness, 5 mm; gap, 1 mm. The total scan time was approximately 12 minutes. The detailed parameters of conventional MR sequences were published previously [16].

2) IVIM-DWI

IVIM-DWI was performed following conventional MRI before radiation and repeatedly at the end of the fifth, 10th, 15th, 20th and 25th fraction of radiations, as well as at the end of IMRT, accompanied by an axial T2-weighted imaging sequence. A single-shot spin-echo echo-planar imaging with 14 b-values (0, 10, 20, 30, 40, 50, 100, 150, 200, 350, 500, 600, 800, and 1,000 sec/mm^2) DWI sequence were acquired with other parameters as follows: TR/TE, 4,495/69 msec; inversion recovery delay, 240 msec; FOV, 23 cm×23 cm; number of signals averaged, 4; matrix, 256×256; thickness, 5 mm; gap, 1 mm; number of slices, 24; three orthogonal diffusion gradients (x, y, z) were turned on simultaneously; scan time, 8 min. The same post-processing of IVIM- DWI has previously been performed [16]. Two experienced radiologists with more than 10-year experience in head and neck MRI conducted the measurement of IVIM parametrics (D, f, and D*) independently, twice, with a double-blind control, in order to minimize the interobserver variability. IVIM parametrics were calculated by using the software termed interactive data language (IDL) (ver. 6.3, ITT Visual Information Solutions, Boulder, Chicago, IL). The regions of interest (ROIs) were firstly contoured manually along the widest cross-section of target lesions on T2WI-STIR image slice, and then subsequently copied and coregistered automatically to IVIM parametric images for analysis with the IDL 6.3 software. The ROI covered at least 2/3 of the area of the target lesions, avoiding the areas of necrosis and adjacent structures (i.e., bone, air, muscles, etc.). IVIM parametrics (D, D*, and f) were extracted using the ROIs defined above.

The formula of the relation between D, D*, and f directly was as follows (Eq. 1):

$$Sb/S0=(1–f)\exp(–bD)+f\exp(–b(D+D^*)) \quad (1)$$

In which D represents the pure diffusion of water molecules in extracellular space, D* represents the perfusion-related diffusion of water molecules in capillary network microcirculation, and f represents the fraction of perfusion-related diffusion.

The baseline D before radiation was noted as D_0, the D from the subsequent Xth fraction was noted as D_X and the end of radiation was D_{end}. The corresponding changes in D (ΔD_X) were calculated using the following equation (Eq. 2):

$$\Delta D_X \text{ (or } \Delta D_{end}) = D_X \text{ (or } D_{end}) - D_0 \quad (2)$$

The relative rates of changes in D_X were defined as δD_X with the following equation (Eq. 3):

$$\delta D_X \text{ (or } \delta D_{end}) = \Delta D_X \text{ (or } \Delta D_{end}) / D_0 \times 100\% \quad (3)$$

The parametrics of D* and f followed the same nomenclature as that employed for D.

3. Evaluation of treatment response

At the end of IMRT and 3 months after all prescriptions of CRT, patients received a routine MRI examination to evaluate the short-term treatment outcomes. Based on the follow-up MRI data and clinical evaluations, patients were classified into responders and non-responders according to the WHO response evaluation criteria in solid tumors [19]. Patients were categorized as responders when all assessable tumors completely disappeared for no less than 4 weeks (complete response [CR]) or when tumor volume (i.e., the longest diameter multiplied by its vertical lengths) decreased by more than 50% for no less than 4 weeks (partial response [PR]). Patients were identified as non-responders if their original tumors showed a < 50% reduction or < 25% increase in tumor volume without any appearance of new lesions (stable disease [SD]) or showed a > 25% increase in tumor volume and/or appearance of new lesions (progressed diseases [PD]).

4. Statistical analyses

The reproducibility of measuring IVIM parametrics was tested by an intra-class correlation coefficient (ICC). One-way ANOVA was applied to analyze the general changes in IVIM parametrics after RT. Student's t-test or the Mann-Whitney U test were conducted to compare parametrics between groups. The receiver operating characteristic (ROC) curve analysis was employed to estimate the diagnostic capability, which was determined by the area under the curve (AUC). All statistical analyses were performed with SPSS ver. 18.0 (SPSS Inc., Chicago, IL).

5. Ethical statement

The Institutional Review Board of Fujian Cancer Hospital approved the protocols of this present study (No. 2015-021-02), and written informed consent was obtained from each participant.

Results

1. The reproducibility of the measurement on IVIM parametrics

The mean value of IVIM parametrics measured by two independent radiologists were treated as the final results of this present study. And the mean value of IVIM parametrics acquired from all recruited patients at the set time points throughout IMRT are shown in Table 2. The overall distribution of D, D*, and f values were consistent with a normal distribution ($p > 0.1$). The inter- and intra-observer ICCs of measurements were for D (0.977 vs. 0.987), f (0.947 vs. 0.964),

Table 2. IVIM parametrics during radiation therapy

Time-point	D ($\times 10^{-3}$ mm^2/sec)	p-value	f (%)	p-value	D* ($\times 10^{-3}$ mm^2/sec)	p-value
Pre-RT	0.928±0.217		0.235±0.013		132.164±0.275	
5th RT	1.038±0.195	0.302	0.252±0.039	0.041	123.216±16.670	0.211
10th RT	1.101±0.232	0.012	0.256±0.045	0.028	121.329±13.777	0.064
15th RT	1.156±0.251	< 0.001	0.247±0.053	0.606	119.627±17.498	0.017
20th RT	1.200±0.219	< 0.001	0.238±0.059	0.909	108.998±16.021	< 0.001
25th RT	1.229±0.219	< 0.001	0.231±0.049	0.365	103.154±16.224	< 0.001
End of RT	1.415±0.346	< 0.001	0.223±0.042	0.048	96.844±16.258	< 0.001

IVIM, intravoxel incoherent motion; RT, radiotherapy.

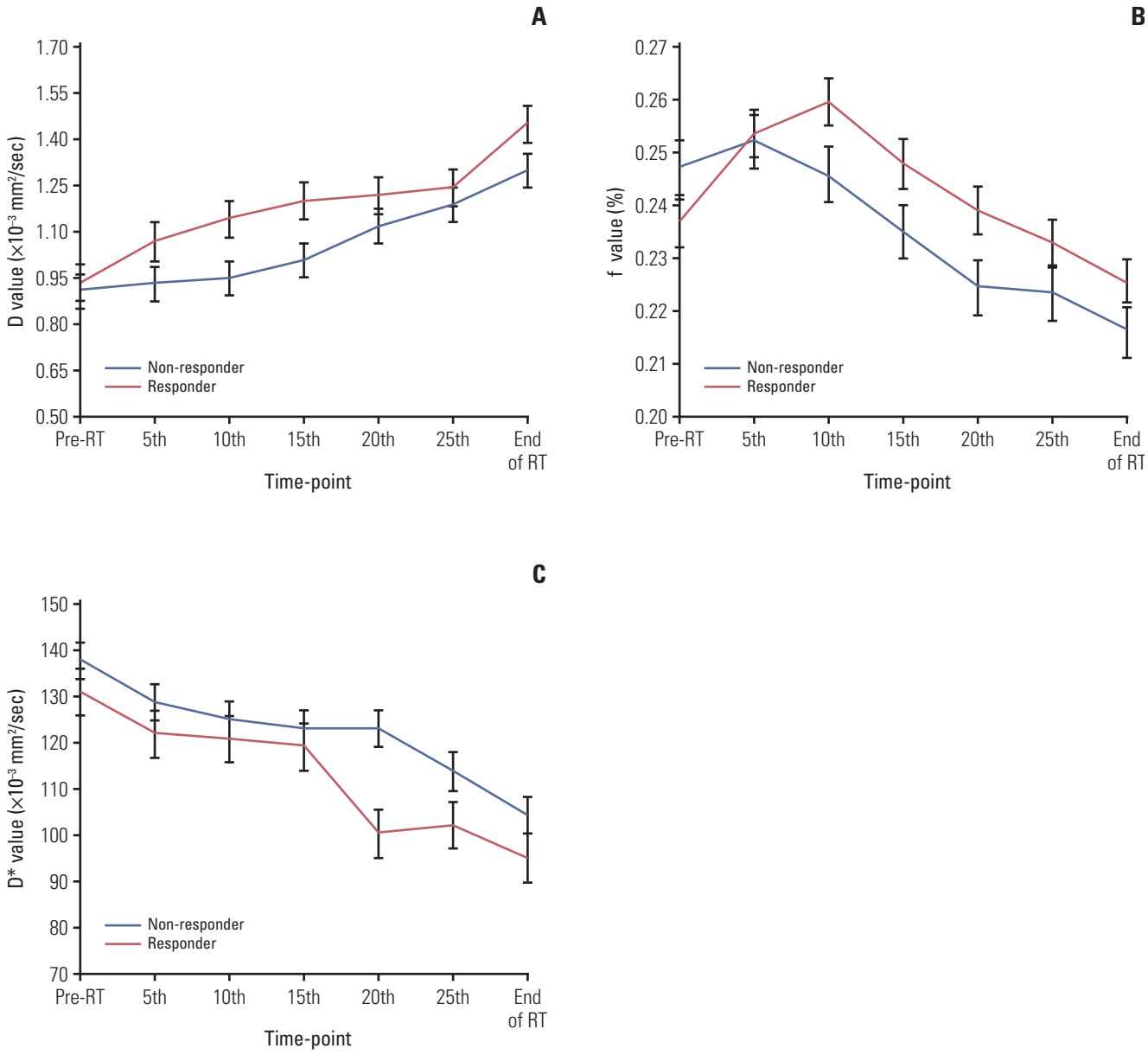

Fig. 1. Comparison of intravoxel incoherent motion parametrics. D (A), f (B), and D* (C) between responders versus non-responders during intensity-modulated radiation therapy. RT, radiotherapy.

and D* (0.883 vs. 0.926); and their corresponding coefficient variations were for D (8.54% vs. 5.83%), f (16.22% vs. 10.60%), and D* (28.69% vs. 19.51%), respectively.

2. IMRT treatment positively influenced IVIM parametrics

The general changes in D, f, and D* after IMRT were statistically significant ($p < 0.001$ for all) (Fig. 1). D were significantly higher after radiations (except D_5; $p=0.302$) than the baseline D_0 ($p < 0.05$), whereas the D* increased significantly compared to D^*_0 ($p < 0.05$), except for D^*_5 ($p=0.211$) and D^*_{10} ($p=0.064$). Moreover, f_5 and f_{10} were significantly higher compared to f_0 ($p < 0.05$), whereas f_{end} was found to be lower than f_0 ($p < 0.05$).

3. IVIM parametrics between responders and non-responders

Based on post-treatment assessment, there were 37 responders (78.72%) and 10 non-responders (21.28%). In particular,

Table 3. IVIM-parametrics coupled with their changes and rates during fractional radiation compared between responders and non-responders

	IVIM parametric			Change (Δ)			Rate (δ)		
	Responder	Non-responder	p-value	Responder	Non-responder	p-value	Responder (%)	Non-responder (%)	p-value
D ($\times 10^{-3}$ mm²/sec)									
D_0	0.933±0.219	0.908±0.217	0.748						
D_5	1.067±0.205	0.933±0.105	0.008	0.134±0.187	0.025±0.261	0.141	17.93	8.23	0.305
D_{10}	1.142±0.235	0.948±0.144	0.003	0.209±0.219	0.040±0.216	0.036	26.76	8.42	0.066
D_{15}	1.197±0.262	1.006±0.123	0.002	0.263±0.298	0.098±0.298	0.127	34.97	17.70	0.25
D_{20}	1.217±0.212	1.116±0.239	0.247	0.283±0.266	0.208±0.262	0.428	37.58	26.64	0.436
D_{25}	1.241±0.210	1.183±0.256	0.524	0.308±0.273	0.275±0.280	0.743	40.33	34.84	0.701
D_{end}	1.447±0.378	1.297±0.147	0.06	0.513±0.428	0.389±0.267	0.387	64.60	49.79	0.512
D* ($\times 10^{-3}$mm²/sec)									
D^*_0	130.587±17.981	137.325±20.344	0.161						
D^*_5	121.653±16.427	128.329±17.210	0.161	–8.934±14.124	–7.845±17.244	0.791	–6.26	–4.80	0.664
D^*_{10}	120.327±12.999	124.609±16.318	0.466	–10.26±18.682	–10.647±21.878	0.973	–6.50	–6.36	0.907
D^*_{15}	118.728±17.596	122.567±17.671	0.33	–28.082±30.894	–14.487±23.827	0.248	–20.14	–9.26	0.205
D^*_{20}	104.832±14.797	122.633±12.138	< 0.001	–25.755±22.636	–13.271±16.123	0.048	–18.29	–8.60	0.041
D^*_{25}	100.001±16.431	113.475±10.623	0.006	–30.586±22.39	–23.084±19.562	0.333	–22.30	–15.55	0.203
D^*_{end}	94.713±27.645	103.818±20.662	0.285	–35.874±28.512	–30.375±17.066	0.511	–26.83	–21.75	0.424
f (%)									
f_0	0.231±0.041	0.250±0.039	0.019						
f_5	0.253±0.041	0.247±0.034	0.927	0.022±0.045	–0.003±0.050	0.137	11.76	1.23	0.192
f_{10}	0.259±0.047	0.242±0.038	0.008	0.028±0.055	–0.008±0.045	0.035	14.98	–1.80	0.079
f_{15}	0.248±0.057	0.242±0.037	0.39	0.017±0.066	–0.008±0.046	0.274	10.06	–1.67	0.276
f_{20}	0.239±0.063	0.235±0.041	0.726	0.008±0.078	–0.017±0.040	0.105	6.96	–7.31	0.166
f_{25}	0.233±0.048	0.225±0.055	0.651	0.002±0.047	–0.025±0.064	0.143	2.46	–8.47	0.195
f_{end}	0.225±0.043	0.217±0.038	0.34	–0.006±0.059	–0.033±0.049	0.284	0.45	–11.66	0.197

IVIM, intravoxel incoherent motion.

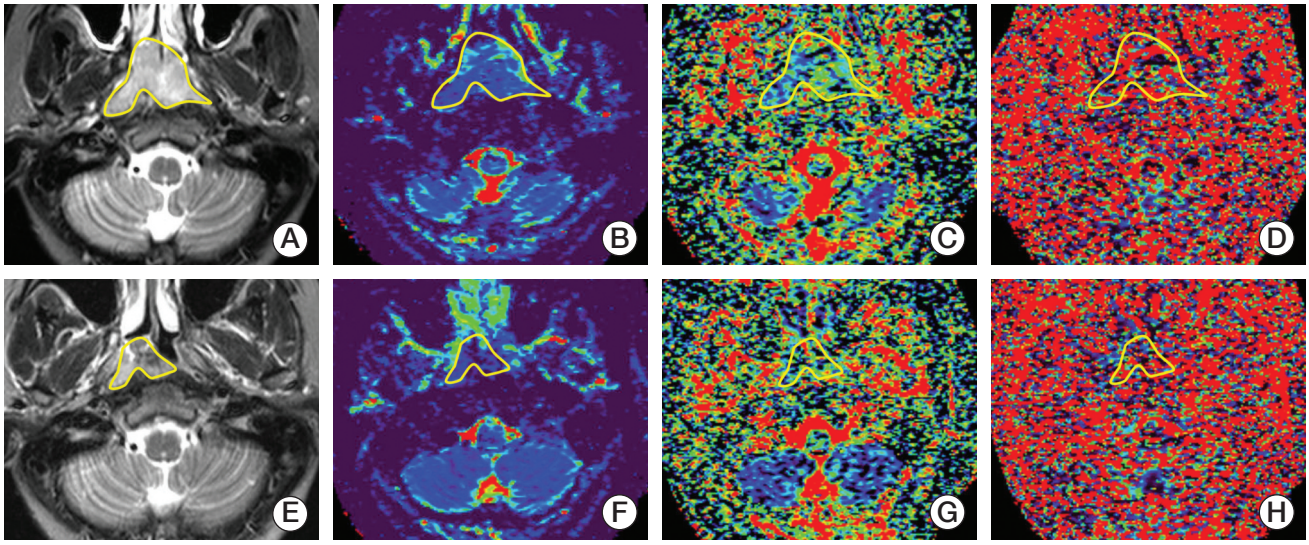

Fig. 2. Intravoxel incoherent motion diffusion-weighted imaging analysis identifies a 37-year-old man with undifferentiated non-keratinizing nasopharyngeal carcinoma as a responder to radiotherapy. The regions of interests (yellow lines) were manually contoured along the bordering of primary nasophayngeal carcinoma on the maps of T2-weighted imaging with short TI inversion recovery (T2WI-STIR) (A), D (B), f (C), and D* (D) before initial radiotherapy, respectively. The baseline D_0, f_0, and D^*_0 are calculated as 0.703×10^{-3} mm^2/sec, 0.238, and 144.623×10^{-3} mm^2/sec, respectively. Maps represent the post-radiation T2WI-STIR (E), D (F), f (G), and D* (H) following the completion of the 15th fraction radiation, and the corresponding D_{15}, f_{15}, and D^*_{15} are measured as 1.216×10^{-3} mm^2/sec, 0.235, and 97.138×10^{-3} mm^2/sec, respectively.

27 cases of CR, 10 cases of PR, nine cases of SD, and one PD were found. The IVIM parametrics of responders and non-responders coupled with their corresponding changes and rates at each time point of IMRT were summarized and compared in Table 3.

Responders presented significantly larger D_5, D_{10}, and D_{15} than non-responders (p=0.008, p=0.003, and p=0.002, respectively). Additionally, the parametrics of f_0, D^*_{20}, and D^*_{25} were significantly larger in responders compared to non-responders (p=0.019, $p < 0.001$, and p=0.006, respectively), whereas the f_{10} of responders was significantly smaller than that for non-responders (p=0.008). Furthermore, significantly larger ΔD_{10} (p=0.036), Δf_{10} (p=0.035), ΔD^*_{20} (p=0.048), and δD^*_{20} (p=0.041) were also observed in responders relative to non-responders (Figs. 2 and 3).

4. The diagnostic capability of IVIM parametrics in differentiating treatment responses

The ROC curve analysis showed that D_5, D_{10}, D_{15}, f_0, f_{10}, D^*_{20}, and D^*_{25} coupled with ΔD_{10}, Δf_{10}, ΔD^*_{20}, and δD^*_{20} could effectively differentiate the treatment responses of IMRT (all $p < 0.05$) (Table 4, Fig. 4) because these parametric values were larger in responders than non-responders (all $p < 0.05$). In particular, D_5, D^*_{20}, and f_{10} differentiated responders from non-responders with their AUC, sensitivity, and specificity values of 0.773, 72.2%, 90.9%; 0.851, 81.8%, 86.1%, and 0.864, 81.8%, 83.3%, respectively (Fig. 4).

1) IVIM parametrics between different treatment regimen groups

All patients were divided into an IMRT alone group, CCRT, and sequential CRT group (NAC+IMRT). The D values of the primary NPC tumor in patients with different CRT regimens were increased after RT, and D increased more gradually in the NAC+RT group. However, the D* and f values decreased, in which the RT group decreased more significantly. D^*_{25} were significantly different when comparing IMRT alone and CCRT groups (p=0.007). However, the difference in D_0, D_{20}, D^*_0, D^*_{25}, and f_{20} between IMRT alone and NAC+IMRT groups was significant (p=0.004, p=0.015, p=0.031, p=0.006, and p=0.034, respectively).

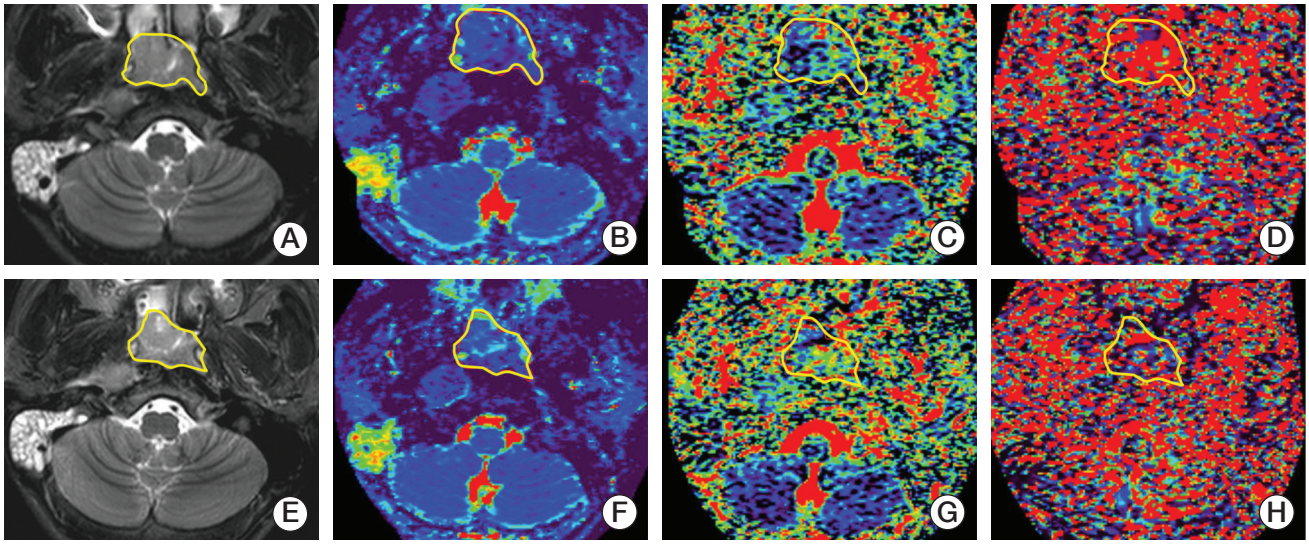

Fig. 3. A 67-year-old male patient with nasopharyngeal carcinoma was identified by intravoxel incoherent motion diffusion-weighted imaging analysis as a non-responder after radiotherapy. Maps depict the baseline T2-weighted imaging with short TI inversion recovery (T2WI-STIR) (A), D (B), f (C), and D* (D) before radiotherapy as well as the T2WI-STIR (E), D (F), f (G), and D* (H) following completion of the 20th fraction radiation. By manually drawing the regions of interest (yellow lines) along the edge of primary nasophayngeal carcinoma, the baseline D_0, f_0, and D^*_0 are calculated as 0.918×10^{-3} mm²/sec, 0.257, and 150.137×10^{-3} mm²/sec, whereas the corresponding D_{20}, f_{20}, and D^*_{20} measured are 1.035×10^{-3} mm²/sec, 0.239, and 133.021×10^{-3} mm²/sec, respectively.

Table 4. The ROC curve analysis of IVIM parametrics

Parametric	AUC	p-value	Threshold	Sensitivity (%)	Specificity (%)
D_5	0.773	0.007	1.013×10^{-3} mm²/sec	0.722	0.909
D_{10}	0.732	0.021	1.132×10^{-3} mm²/sec	0.472	1.000
D_{15}	0.765	0.008	1.179×10^{-3} mm²/sec	0.528	0.909
D^*_{20}	0.851	< 0.001	114.700×10^{-3} mm²/sec	0.818	0.833
D^*_{25}	0.756	0.011	106.835×10^{-3} mm²/sec	0.818	0.694
f_0	0.731	0.022	0.241	1.000	0.417
f_{10}	0.864	< 0.001	0.255	0.818	0.861
ΔD_{10}	0.726	0.030	0.006×10^{-3} mm²/sec	0.892	0.500
Δf_{10}	0.689	0.039	0.053	0.378	1.000
ΔD^*_{20}	0.703	0.034	-23.850×10^{-3} mm²/sec	0.900	0.541
δD^*_{20}	0.732	0.021	17.03%	0.900	0.622

ROC, receiver operating characteristic; IVIM, intravoxel incoherent motion; AUC, area under the curve.

Discussion

The current study investigated the assessment of treatment responses in NPC by IVIM-DWI. IVIM parametrics including D, f, and D* altered significantly for responders during the course of IMRT. In particular, D and f were more sensitive to assess response in the early course of the treatment, whereas D* revealed changes in later stages.

The bi-exponential model of IVIM demonstrated the heterogeneity of water diffusion and differentiated the contributions from perfusion from diffusion [9,10,20]. Compared to conventional ADC measurement by DWI, IVIM parametrics can simultaneously and separately quantify tissue perfusion and diffusion, and better characterize the pathological features of tumor tissues as well as their response to chemo-

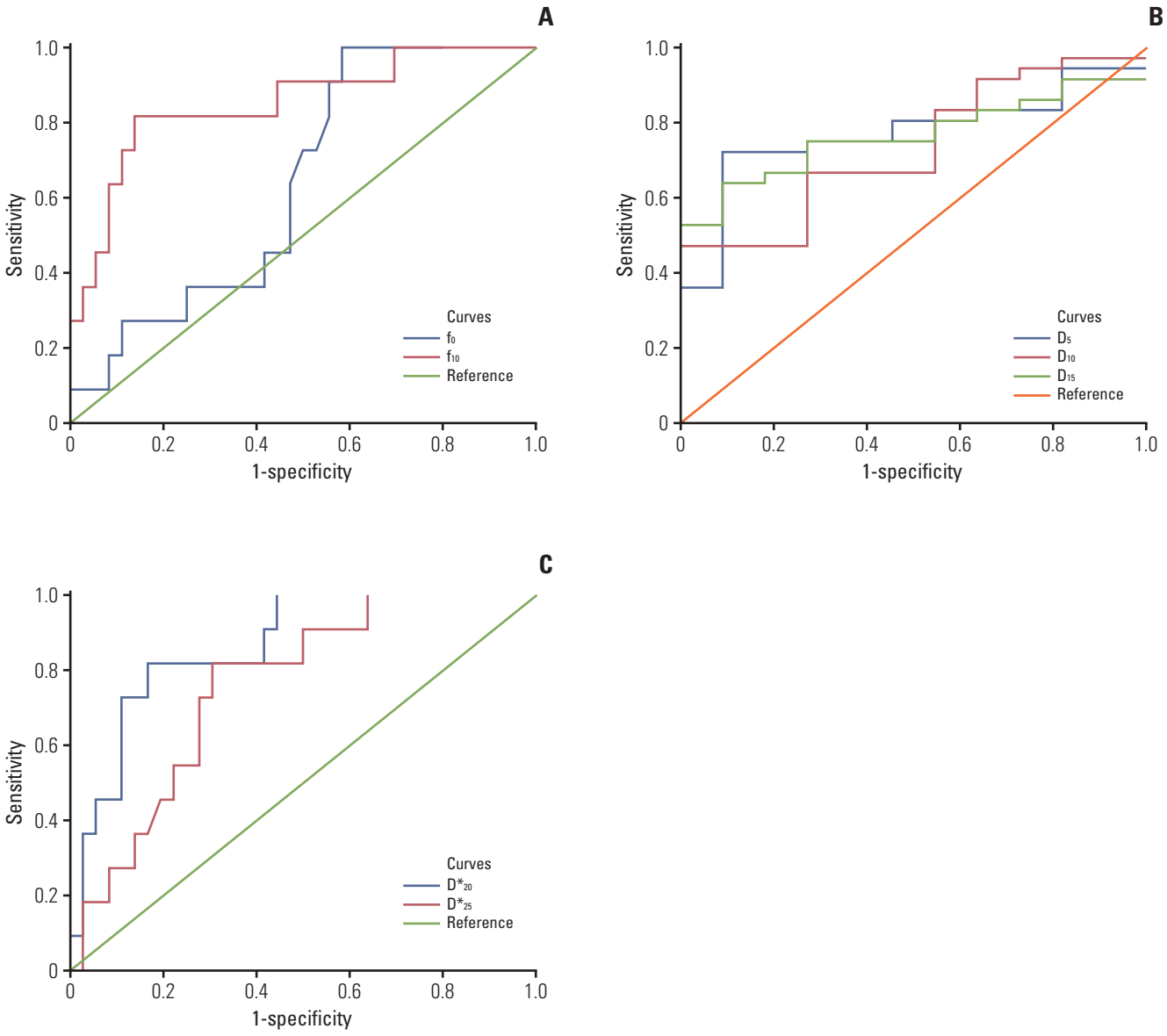

Fig. 4. The receiver operating characteristic curves of intravoxel incoherent motion parametrics. D (A), f (B), and D* (C) in predicting tumor responsiveness to radiotherapy.

radiotherapy. Upon radiation therapy, large numbers of tumor cells underwent apoptosis, resulting in a higher degree of fluid migration into the extracellular space (i.e., pure diffusion). Meanwhile, the obstruction of microcirculation became severe, leading to less blood flow in capillary networks (i.e., pseudo-diffusion). Both the cellularity and immature microvessels in tumor tissues decreased dramatically. The overall effect of these pathological events led to a significant increase in D as well as decrease in D*, which were found in our data. Lai et al. [12] reported a similar diffusion perfusion change in residual NPC tumors after RT compared with post-radiation fibrosis. Furthermore, both D and D* were found to be significantly altered in responders relative to non-responders, indicating their potential in predicting the short-term treatment response of NPC [21-25].

Recent studies have employed diffusion MRI to monitor the treatment response of tumors in CRT [21-23]. Our previous study also demonstrated that NPC with a lower baseline D_0, which had a higher cellularity, responded better to NAC [16]. Because D composes diffusion in the extracellular and intracellular space, an alteration in D reflected the microstructure changes for the assessment of the treatment respon-

se in IMRT. This was consistent with Mardor et al.'s study [24] showing that both ADC and R_D (a diffusion index indicates the normalized summation of signal decay) before treatment were closely correlated with tumor radio-sensitivity. Although there were no significant changes in D after the fifth fraction, the D_5 of responders was significantly larger than that of non-responders. ROC analysis suggested that D_5 could differentiate treatment responses with AUC, sensitivity, and specificity of 0.773, 72.2%, and 90.9%, respectively. Lu et al. [25] also reported that HNSCC patients with a lower standard deviation of pre-treatment D responded better to treatment. Similar, studies also demonstrated the prognostic value of D [16,21-25]. However, perfusion measured by MRI has been used to assess the therapeutic effects and long-term prognosis for patients with malignancies. The perfusion level of tissues was suggested to potentially predict the tumor sensitivity of CRT [26,27]. Lai et al. [12,13] reported that f could effectively distinguish residual tumors of NPC from radiation-related fibrous tissues, as well as tumor stages. HNSCC patients with a smaller perfusion fraction were always accompanied with a low survival rate [22]. Interestingly, our present results showed that responders expressed a smaller baseline f_0, a larger f_{10} and Δf_{10} relative to non-responders. These may infer the irradiation damages on the integrity of microvascular walls in the early course of IMRT.

D and f were more sensitive in the early course of treatment, whereas D* changes more in later course in responders relative to non-responders. The ROC curve analysis further illustrated that D_5, D^*_{20}, and f_{10} better differentiate responders from non-responders. These findings may indicate that the destruction of cell structures by irradiations in radio-sensitive tumors was more predominant early in the treatment, whereas damage to microcirculation was more evident at the later course of radiation. Larocque et al. [28] and Koh [29] both demonstrated that early changes in diffusion parametrics could be used to evaluate the sensitivity of RT and/or chemotherapy. They observed that the average tumor ADC value increased significantly 7 days after irradiation [28] and that the correlation between the decrease in perfusion parametrics (D* and f) and tumor shrinkage 7 days after treatment significantly increased [29]. Hong et al. [8] also suggested ADC to predict the short-term treatment response to RT in NPC. All of the above supported that the IVIM parametrics reflect tumor intrinsic radiosensitivity and biological response.

Additionally, IVIM parametrics could indicate a response of various treatment regimens (i.e., IMRT with or without neoadjuvant or concurrent chemotherapy). D_0 of the NAC+IMRT group was significantly larger than IMRT alone and CCRT, whereas D^*_0 of the NAC+IMRT group was significantly smaller than those of the latter. The D_{20}, f_{20}, and D^*_{25} parametrics between IMRT alone and NAC+IMRT groups were significantly different, whereas D^*_{25} was significantly different between IMRT alone and the CCRT groups. These indicated a significant increase in D and decrease in D* caused by NAC. This could be attributed to a decrease the cellularity and increase extracellular space upon NAC. Additionally, a decrease in tumor perfusion may suggest microcirculation blockage, which in turn influences the oxygen metabolism of tumor cells and the radio-sensitivity of NPC. No significant difference was found in IVIM parametrics between NAC+IMRT and CCRT throughout the course of treatment. This may suggest similar cytotoxic effects on tumor cells between neoadjuvant and concurrent chemotherapy.

To further solidify the evidence presented in this study, additional examinations will be assessed. First, histopathological examinations during radiations were not obtained for ethical reasons. Complementary studies on NPC xenografts are needed to analyze the pathological changes during fractional radiations. Second, the current study only evaluated local control and short-term treatment outcomes of primary NPC tumors, while initial staging (such as WHO grades and nodal or distant metastasis) was not considered between responders and non-responders. Nevertheless, the latest follow-up data indicated that three cases of local and regional relapse and two cases of distant metastases were all found in non-responders rather than responders. In this regard, a prospective study with a prolonged follow-up period to investigate the long-term survival of patients and cancer staging would be possible. Lastly, the sample size of this prospective study was relatively small, which should be expanded.

Compared to non-responders, responders presented significantly larger changes in D and f at the early course of treatment and D* later in the treatment. IVIM-DWI could effectively assess the short-term treatment response to RT and could be recommended to predict the radiosensitivity of NPCs.

Conflicts of Interest

Conflict of interest relevant to this article was not reported.

Acknowledgments

This study was supported by the Medical Union Project of Fujian Province Natural Science Foundation (Grant No.2016J01438) and was partly supported by the National Clinical Key Specialty Construction Program and Key Clinical Specialty Discipline Construction Program of Fujian Province, P.R.C.

References

1. Chua ML, Wee JT, Hui EP, Chan AT. Nasopharyngeal carcinoma. Lancet. 2016;387:1012-24.
2. World Health Organization. GLOBOCAN 2012 v1.0, Estimated cancer incidence, mortality and prevalence worldwide in 2012: IARC Cancer Base No. 11 [Internet]. Lyon: International Agency for Research on Cancer; 2012 [cited 2017 Dec 12]. Available from: http://globocan.iarc.fr/Default.aspx.
3. Su SF, Han F, Zhao C, Chen CY, Xiao WW, Li JX, et al. Long-term outcomes of early-stage nasopharyngeal carcinoma patients treated with intensity-modulated radiotherapy alone. Int J Radiat Oncol Biol Phys. 2012;82:327-33.
4. Lee AW, Ng WT, Chan LL, Hung WM, Chan CC, Sze HC, et al. Evolution of treatment for nasopharyngeal cancer: success and setback in the intensity-modulated radiotherapy era. Radiother Oncol. 2014;110:377-84.
5. Song JH, Wu HG, Keam BS, Hah JH, Ahn YC, Oh D, et al. The role of neoadjuvant chemotherapy in the treatment of nasopharyngeal carcinoma: a multi-institutional retrospective study (KROG 11-06) using propensity score matching analysis. Cancer Res Treat. 2016;48:917-27.
6. Chen YP, Wang ZX, Chen L, Liu X, Tang LL, Mao YP, et al. A Bayesian network meta-analysis comparing concurrent chemoradiotherapy followed by adjuvant chemotherapy, concurrent chemoradiotherapy alone and radiotherapy alone in patients with locoregionally advanced nasopharyngeal carcinoma. Ann Oncol. 2015;26:205-11.
7. Chen L, Hu CS, Chen XZ, Hu GQ, Cheng ZB, Sun Y, et al. Concurrent chemoradiotherapy plus adjuvant chemotherapy versus concurrent chemoradiotherapy alone in patients with locoregionally advanced nasopharyngeal carcinoma: a phase 3 multicentre randomised controlled trial. Lancet Oncol. 2012;13:163-71.
8. Hong J, Yao Y, Zhang Y, Tang T, Zhang H, Bao D, et al. Value of magnetic resonance diffusion-weighted imaging for the prediction of radiosensitivity in nasopharyngeal carcinoma. Otolaryngol Head Neck Surg. 2013;149:707-13.
9. Le Bihan D, Breton E, Lallemand D, Grenier P, Cabanis E, Laval-Jeantet M. MR imaging of intravoxel incoherent motions: application to diffusion and perfusion in neurologic disorders. Radiology. 1986;161:401-7.
10. Le Bihan D, Breton E, Lallemand D, Aubin ML, Vignaud J, Laval-Jeantet M. Separation of diffusion and perfusion in intravoxel incoherent motion MR imaging. Radiology. 1988;168:497-505.
11. Sasaki M, Sumi M, Eida S, Katayama I, Hotokezaka Y, Nakamura T. Simple and reliable determination of intravoxel incoherent motion parameters for the differential diagnosis of head and neck tumors. PLoS One. 2014;9:e112866.
12. Lai V, Li X, Lee VH, Lam KO, Chan Q, Khong PL. Intravoxel incoherent motion MR imaging: comparison of diffusion and perfusion characteristics between nasopharyngeal carcinoma and post-chemoradiation fibrosis. Eur Radiol. 2013;23:2793-801.
13. Lai V, Li X, Lee VH, Lam KO, Fong DY, Huang B, et al. Nasopharyngeal carcinoma: comparison of diffusion and perfusion characteristics between different tumour stages using intravoxel incoherent motion MR imaging. Eur Radiol. 2014;24:176-83.
14. Hauser T, Essig M, Jensen A, Laun FB, Munter M, Maier-Hein KH, et al. Prediction of treatment response in head and neck carcinomas using IVIM-DWI: evaluation of lymph node metastasis. Eur J Radiol. 2014;83:783-7.
15. Cui Y, Zhang C, Li X, Liu H, Yin B, Xu T, et al. Intravoxel incoherent motion diffusion-weighted magnetic resonance imaging for monitoring the early response to ZD6474 from nasopharyngeal carcinoma in nude mouse. Sci Rep. 2015;5:16389.
16. Xiao Y, Pan J, Chen Y, Chen Y, He Z, Zheng X. Intravoxel incoherent motion-magnetic resonance imaging as an early predictor of treatment response to neoadjuvant chemotherapy in locoregionally advanced nasopharyngeal carcinoma. Medicine (Baltimore). 2015;94:e973.
17. Edge SB, Compton CC. The American Joint Committee on Cancer: the 7th edition of the AJCC cancer staging manual and the future of TNM. Ann Surg Oncol. 2010;17:1471-4.
18. Lin S, Pan J, Han L, Zhang X, Liao X, Lu JJ. Nasopharyngeal carcinoma treated with reduced-volume intensity-modulated radiation therapy: report on the 3-year outcome of a prospective series. Int J Radiat Oncol Biol Phys. 2009;75:1071-8.
19. Khokher S, Qureshi MU, Chaudhry NA. Comparison of WHO and RECIST criteria for evaluation of clinical response to chemotherapy in patients with advanced breast cancer. Asian Pac J Cancer Prev. 2012;13:3213-8.
20. Le Bihan D. Diffusion, confusion and functional MRI. Neuroimage. 2012;62:1131-6.
21. Pan J, Zang L, Zhang Y, Hong J, Yao Y, Zou C, et al. Early changes in apparent diffusion coefficients predict radiosensitivity of human nasopharyngeal carcinoma xenografts. Laryngoscope. 2012;122:839-43.
22. Chawla S, Kim S, Dougherty L, Wang S, Loevner LA, Quon H, et al. Pretreatment diffusion-weighted and dynamic contrast-enhanced MRI for prediction of local treatment response in squamous cell carcinomas of the head and neck. AJR Am J Roentgenol. 2013;200:35-43.
23. Chen Y, Liu X, Zheng D, Xu L, Hong L, Xu Y, et al. Diffusion-weighted magnetic resonance imaging for early response assessment of chemoradiotherapy in patients with nasopharyngeal carcinoma. Magn Reson Imaging. 2014;32:630-7.
24. Mardor Y, Roth Y, Ochershvilli A, Spiegelmann R, Tichler T, Daniels D, et al. Pretreatment prediction of brain tumors' response to radiation therapy using high b-value diffusion-weighted MRI. Neoplasia. 2004;6:136-42.
25. Lu Y, Jansen JF, Stambuk HE, Gupta G, Lee N, Gonen M, et al. Comparing primary tumors and metastatic nodes in head and neck cancer using intravoxel incoherent motion imaging: a preliminary experience. J Comput Assist Tomogr. 2013;37:346-52.
26. Bisdas S, Braun C, Skardelly M, Schittenhelm J, Teo TH, Thng

CH, et al. Correlative assessment of tumor microcirculation using contrast-enhanced perfusion MRI and intravoxel incoherent motion diffusion-weighted MRI: is there a link between them? NMR Biomed. 2014;27:1184-91.
27. King AD, Chow SK, Yu KH, Mo FK, Yeung DK, Yuan J, et al. DCE-MRI for pre-treatment prediction and post-treatment assessment of treatment response in sites of squamous cell carcinoma in the head and neck. PLoS One. 2015;10:e0144770.
28. Larocque MP, Syme A, Allalunis-Turner J, Fallone BG. ADC response to radiation therapy correlates with induced changes in radiosensitivity. Med Phys. 2010;37:3855-61.
29. Koh DM. Science to practice: can intravoxel incoherent motion diffusion-weighted MR imaging be used to assess tumor response to antivascular drugs? Radiology. 2014;272:307-8.